

Robust Model Predictive Control with State Estimation under Set-Membership Uncertainty

Tianchen Ji¹, Junyi Geng², and Katherine Driggs-Campbell¹

Abstract—Robust design of autonomous systems under uncertainty is an important and challenging problem. In practice, state disturbances and state estimation error may cause a controller to fail to accomplish its task or even to stabilize the system. In this paper, we propose a novel tube-based robust model predictive control design based on set-membership state estimation for constrained systems with unknown but bounded state and output disturbances. With more accurate and efficient error bounding methods, the proposed controller ensures robust constraint satisfaction, guarantees recursive feasibility and stability, generates less conservative behavior than the previous work, and scales well to high-dimensional robotic applications. Our simulated experiments on three different systems (double integrator, robotic walker, and quadrotor) demonstrate that the proposed controller is robust against a larger range of disturbances and results in superior closed-loop performance than baseline methods.

I. INTRODUCTION

Model predictive control (MPC) is a feedback control technique based on the iterative solution of an optimization problem [1]. By using a predictive model of the system and the current state information, MPC plans the optimal control sequence based on the cost function. The system executes the first control action in the optimal sequence and the procedure repeats at the next sampling time. MPC has received considerable attention over the last decades driven largely by its ability to handle multi-variable systems and hard constraints on states and control actions [2].

In practice, however, two important issues arise in MPC design: (i) actual system states are not available as feedback signals, leading to the necessity of state estimation, and (ii) measurements and the model used for prediction are uncertain (e.g., due to unmodeled dynamics and disturbances) [3]. A simple way to apply MPC on uncertain systems is by employing ‘certainty equivalence’, i.e., designing a deterministic/nominal MPC with the state estimates in replacement of the actual states. However, the stability of such closed-loop uncertain system cannot be ensured by simply combining a stable estimator with the nominal MPC [4]–[6].

To overcome this problem, extensive research has focused on robust MPC design that takes the state estimation error directly into account, dating back to the early 2000s. Bemporad and Garulli [7] combined predictive control and the minimum volume parallelotopic state estimation to achieve

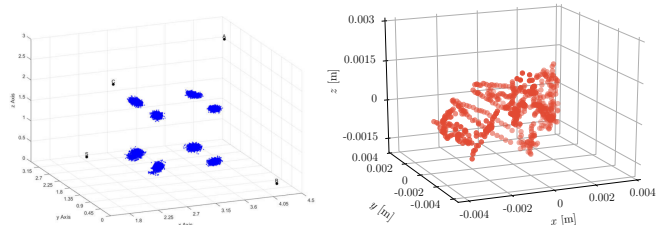


Fig. 1: Real disturbances in different systems turn out to lie in ellipsoidal bounding sets. *Left* [11]: Measurements for eight different test points from Decawave indoor positioning system. Blue dots indicate the measurement results and black dots indicate the places of anchors. *Right*: RTK GPS position measurements on a static Polaris GEM autonomous vehicle [12]. The measurements have been normalized to have zero mean.

robust constraint satisfaction for uncertain systems. Chisci and Zappa [8] adopted the Kalman filter as the state estimator to design the robust controller. Mayne et al. [6], [9] constructed the robust output feedback MPC as a combination of a stable Luenberger observer, whose estimation error is bounded by an invariant set, and a tube-based predictive controller which ensures that all possible realizations of the state trajectory lie in an uncertainty tube. In recent years, Le et al. [10] realized the state estimation using a zonotopic set-membership estimation, then a tube-based MPC is designed in a similar manner to [9]. The output feedback MPC developed by Qiu et al. [2] employed an ellipsoidal state estimation and incorporated the system constraints into LMI conditions such that the control actions can be computed by using semi-definite programming.

However, these approaches may suffer from high computational complexity [7], [10], rely on probabilistic assumptions on disturbances which are hard to validate [8], generate conservative closed-loop behavior under large disturbances [6], [9], or lacks guarantees on recursive feasibility and stability [2]. Furthermore, all the above methods were only validated on two-dimensional systems and the generalization of these methods to high-dimensional systems remains unclear.

In robust MPC literature, bounding sets for disturbances are often described as boxes or polytopes due to the resulting simplicity of bounding errors for controllers [3], [9], [10], [13], [14]. Through real experiments, however, ellipsoids turn out to be a more suitable description of uncertainty for noises (Figure 1). As a result, we adopt ellipsoidal set-membership state estimation, which has another advantage of lower computational complexity than parallelotopic state estimation in terms of updating the state uncertainty sets [15]–[18].

We consider the robust output feedback problem for constrained linear systems subject to state and measurement disturbances. The design procedure of our controller in the

¹T. Ji and K. Driggs-Campbell are with the Department of Electrical and Computer Engineering at the University of Illinois at Urbana-Champaign. emails: {tj12,krdc}@illinois.edu

²Junyi Geng is with the Robotics Institute at the Carnegie Mellon University. email: junyigen@andrew.cmu.edu

paper is as follows: (i) the set-membership state estimation error is bounded by a precomputable set (Section III-A); (ii) the control error is subsequently bounded by a precomputable invariant set (Section III-B); and (iii) by using the bounding sets of the estimation and control error, the ‘cross-section’ of the trajectory tube can be computed and the ‘center’ of the tube (the nominal state) can then be optimized based on the cost function while ensuring that the entire tube satisfies all the constraints on the original system (Section IV). Since all possible realizations of the state trajectory lie in the trajectory tube, the constraint satisfaction can be guaranteed for all admissible disturbance sequences.

Using the novel state decomposition method and the simplicity of the computation of error bounding sets, the proposed controller ensures robust constraint satisfaction, guarantees recursive feasibility and stability, has comparable computational complexity to nominal MPC, and scales well to high-dimensional systems. Moreover, the theory and the simulation examples both indicate that the resulting controller generates less conservative closed-loop behavior and adapts to larger range of disturbances compared to existing methods [6], [9]. Although we focus on linear systems in this paper, the extension to the control of a class of nonlinear systems using the proposed controller is also achievable by applying state feedback linearization [19]–[21].

Nomenclature: In the following sections, $\mathbb{N} := \{0, 1, 2, \dots\}$ and $\mathbb{R}_+ = \{x \in \mathbb{R} \mid x \geq 0\}$. A set $\mathcal{U} \subset \mathbb{R}^n$ is a C set if it is compact, convex, and contains the origin in its non-empty interior. Let $\rho(A)$ denote the spectral radius of a given matrix $A \in \mathbb{R}^{n \times n}$. Given two sets $\mathcal{U} \subset \mathbb{R}^n$ and $\mathcal{V} \subset \mathbb{R}^n$, Minkowski sum is defined by $\mathcal{U} \oplus \mathcal{V} := \{u + v \mid u \in \mathcal{U}, v \in \mathcal{V}\}$ and Minkowski difference by $\mathcal{U} \ominus \mathcal{V} := \{x \mid x \oplus \mathcal{V} \subset \mathcal{U}\}$. Hereafter, the maximization of a vector-valued function is to be performed elementwise.

II. PROBLEM FORMULATION AND BACKGROUND

In the following section, we introduce the robust optimal control problem of constrained linear systems and describe the set-membership state estimation algorithm.

A. Robust Constrained Optimal Control

We consider the following uncertain discrete-time linear time-invariant system:

$$\begin{aligned} x_{t+1} &= Ax_t + Bu_t + Dw_t, & x_0 &= x_S, \\ y_t &= Cx_t + v_t, \end{aligned} \quad (1)$$

where $x_t \in \mathbb{R}^n$ is the system state at time t , x_S is an initial state, $u_t \in \mathbb{R}^m$ is the control action, $w_t \in \mathbb{R}^q$ is an unknown state disturbance, $y_t \in \mathbb{R}^p$ is the measured output, $v_t \in \mathbb{R}^p$ is an unknown output disturbance, and $(A, B, C, D) \in \mathbb{R}^{n \times n} \times \mathbb{R}^{n \times m} \times \mathbb{R}^{p \times n} \times \mathbb{R}^{n \times q}$ are known matrices, where the couple (A, B) is assumed to be controllable and (A, C) observable. At each time t , the additive state and output disturbances w_t and v_t are only known to the extent that they lie, respectively, in the C sets $\mathbb{W} \subset \mathbb{R}^q$ and $\mathbb{V} \subset \mathbb{R}^p$: $(w_t, v_t) \in \mathbb{W} \times \mathbb{V}$, $\forall t \in \mathbb{N}$. System (1) is subject to the following mixed constraints

on the states and control actions:

$$Fx_t + Gu_t \leq f, \quad (2)$$

where $(F, G, f) \in \mathbb{R}^{d \times n} \times \mathbb{R}^{d \times m} \times \mathbb{R}^d$ are known matrices. In order to counteract the disturbances, the control action is a feedback policy $u_t(\cdot)$ with state estimate $\hat{x}_t \in \mathbb{R}^n$ as the feedback signal, where $u_t(\hat{x}_t) \in \mathbb{R}^m$.

To evaluate the predicted performance of uncertain systems, we consider the nominal cost corresponding to the case of no model uncertainty, i.e., $w_t = 0$, $\forall t \in \mathbb{N}$. Our goal is to design a controller that solves the following infinite horizon robust constrained optimal control problem:

$$\begin{aligned} V_\infty^*(\hat{x}_0) &= \min_{\mathbf{u}(\cdot)} \sum_{t=0}^{\infty} q(s_t, u_t(s_t)) \\ \text{s.t.} \quad & s_{t+1} = As_t + Bu_t(s_t), \quad s_0 = \hat{x}_0, \\ & x_{t+1} = Ax_t + Bu_t(\hat{x}_t) + Dw_t, \quad x_0 = x_S, \\ & Fx_t + Gu_t(\hat{x}_t) \leq f, \quad \forall w_t \in \mathbb{W}, \forall v_t \in \mathbb{V}, \\ & t = 0, 1, 2, \dots, \end{aligned} \quad (3)$$

where $\mathbf{u}(\cdot) := \{u_0(\cdot), u_1(\cdot), \dots\}$ is the sequence of feedback policies, $s_t \in \mathbb{R}^n$ is the nominal state, and $q: \mathbb{R}^n \times \mathbb{R}^m \mapsto \mathbb{R}_+$ is a positive definite stage cost. Note that only the state estimate rather than the true state is available to the controller. The output disturbance v_t implicitly affects the system through the feedback control $u_t(\hat{x}_t)$ as the state estimate \hat{x}_t is a function of the output y_t at time t . The key challenge here is to design a robust controller such that the constraint (2) is satisfied for all admissible disturbance sequences $\mathbf{w} := \{w_0, w_1, \dots\}$ and $\mathbf{v} := \{v_0, v_1, \dots\}$.

The optimization problem (3) is intractable because: (i) the optimization is performed over the infinite-dimensional space of all feedback policies; and (ii) the horizon is infinite. In this paper, we adopt control policy approximation to convert the infinite horizon robust optimal control problem to a tractable finite horizon problem and apply the receding horizon control strategy to control the system [13], [22].

B. Set-Membership State Estimation

In order to estimate the state, a recursive set-membership state estimation algorithm is employed [16], [23]. Hereafter, we shall assume that the uncertainty sets \mathbb{W} and \mathbb{V} are described as ellipsoids:

$$w_t \in \mathbb{W} := \{w \mid w^\top Q^{-1} w \leq 1\}, \quad \forall t \in \mathbb{N}, \quad (4a)$$

$$v_t \in \mathbb{V} := \{v \mid v^\top R^{-1} v \leq 1\}, \quad \forall t \in \mathbb{N}, \quad (4b)$$

where Q and R are known positive definite matrices. Moreover, the initial state is bounded by a given ellipsoid:

$$x_0 \in \mathbb{X}_0 := \{x \mid (x - \hat{x}_0)^\top \Psi^{-1} (x - \hat{x}_0) \leq 1\}, \quad (5)$$

where \hat{x}_0 is a given initial guess of x_0 and Ψ is a known positive definite matrix. For the sake of completeness, we outline the discrete time set-membership state estimation algorithm developed by Bertsekas and Rhodes [16].

Recursive Set-Membership State Estimation: Given the system (1), the disturbance bounds (4), and the initial state

bound (5), a bounding set $X_{t|t}$ to the set of all possible states x_t at time t given the outputs observed up to time t can be described as an ellipsoid:

$$X_{t|t} = \{x \mid (x - \hat{x}_t)^\top P_{t|t}^{-1} (x - \hat{x}_t) \leq 1 - \delta_t^2\}, \quad (6)$$

where the positive definite matrix $P_{t|t}$ is recursively given by the equations:

$$\begin{aligned} P_{t+1|t+1} &= [(1-\rho)P_{t+1|t}^{-1} + \rho C^\top R^{-1} C]^{-1}, \\ P_{t+1|t} &= (1-\beta)^{-1} A P_{t|t} A^\top + \beta^{-1} D Q D^\top, \\ P_{0|0} &= \Psi. \end{aligned} \quad (7)$$

The estimate \hat{x}_t evolves according to:

$$\hat{x}_{t+1} = A\hat{x}_t + B u_t + \rho P_{t+1|t+1} C^\top R^{-1} (y_{t+1} - C(A\hat{x}_t + B u_t)) \quad (8)$$

with \hat{x}_0 as the initial condition and the non-negative real number δ_t^2 is given by the equation:

$$\begin{aligned} \delta_{t+1}^2 &= (1-\beta)(1-\rho)\delta_t^2 \\ &\quad + (y_{t+1} - C(A\hat{x}_t + B u_t))[(1-\rho)^{-1} C P_{t+1|t} C^\top \\ &\quad + \rho^{-1} R]^{-1} (y_{t+1} - C(A\hat{x}_t + B u_t)), \\ \delta_0^2 &= 0, \end{aligned} \quad (9)$$

where β, ρ are parameters with $0 < \beta < 1$ and $0 < \rho < 1$.

We point out two desirable properties of the state estimation algorithm given by (6)–(9):

- i) The matrix $P_{t|t}$ does not depend on the outputs along the trajectory, and hence can be precomputed.
- ii) In cases of time-invariant systems with (A, B) controllable and (A, C) observable, the solution to (7) goes to a steady state as time goes to infinity, i.e., $P_{t|t} \rightarrow P_\infty$ as $t \rightarrow \infty$. We refer to [16] for detailed proof.

The above two properties will be helpful to compute bounds for the estimation error and subsequently the control error while planning the optimal control actions.

Note that the time indices used in Section II-A and Section II-B do not need to match in practice. For example, the state estimation can start running before control is applied, in which case the initial state in control could be the steady state in state estimation.

III. BOUNDING ESTIMATION AND CONTROL ERRORS

In this section, we extend the set-membership state estimation algorithm (Section II-B) to compute bounds for the estimation error over the prediction horizon and adopt the state decomposition method to compute bounds for the control error.

A. Bounding the Estimation Error

We present the following proposition bounding the estimation error $\varepsilon_t := \hat{x}_t - x_t$ without prior knowledge of the subsequent system outputs.

Proposition III.1. *Consider the set-membership state estimation (6)–(9) associated with the system (1). At time t , it is guaranteed that the estimation error in the next k steps $\varepsilon_{t+k} \in \mathbb{E}_{t+k|t} := \{\varepsilon \mid \varepsilon^\top P_{t+k|t+k}^{-1} \varepsilon \leq 1 - (1-\beta)^k (1-\rho)^k \delta_t^2\}$ for all $t \in \mathbb{N}$, all $k \in \mathbb{N}$, and all*

admissible disturbance sequences \mathbf{w} and \mathbf{v} , where $\mathbb{E}_{t+k|t}$ is the bounding ellipsoid of the estimation error at time $t+k$ based on the information available at time t .

Proof. Given the information available at time t , we first prove by induction that $\delta_{t+k}^2 \geq (1-\beta)^k (1-\rho)^k \delta_t^2$ for all $k \in \mathbb{N}$. Clearly, $k=0$ satisfies the inequality. Assume that $\delta_{t+k}^2 \geq (1-\beta)^k (1-\rho)^k \delta_t^2$. From (9), we then have:

$$\begin{aligned} \delta_{t+k+1}^2 &= (1-\beta)(1-\rho)\delta_{t+k}^2 + (y_{t+k+1} \\ &\quad - C(A\hat{x}_{t+k} + B u_{t+k}))[(1-\rho)^{-1} C P_{t+k+1|t+k} C^\top \\ &\quad + \rho^{-1} R]^{-1} (y_{t+k+1} - C(A\hat{x}_{t+k} + B u_{t+k})) \\ &\geq (1-\beta)(1-\rho)\delta_{t+k}^2 \\ &\geq (1-\beta)^{k+1} (1-\rho)^{k+1} \delta_t^2 \end{aligned}$$

by the fact that $[(1-\rho)^{-1} C P_{t+k+1|t+k} C^\top + \rho^{-1} R]^{-1}$ is positive definite¹ and that $0 < \beta < 1$, $0 < \rho < 1$. Thus, we conclude that $\delta_{t+k}^2 \geq (1-\beta)^k (1-\rho)^k \delta_t^2$ for all $k \in \mathbb{N}$. From (6), for all $x_{t+k} \in X_{t+k|t+k}$, we have that:

$$\begin{aligned} (x_{t+k} - \hat{x}_{t+k})^\top P_{t+k|t+k}^{-1} (x_{t+k} - \hat{x}_{t+k}) \\ \leq 1 - \delta_{t+k}^2 \leq 1 - (1-\beta)^k (1-\rho)^k \delta_t^2. \end{aligned}$$

By definition of the estimation error ε_t , we then have $\varepsilon_{t+k}^\top P_{t+k|t+k}^{-1} \varepsilon_{t+k} \leq 1 - (1-\beta)^k (1-\rho)^k \delta_t^2$ for all $k \in \mathbb{N}$, which completes the proof. ■

Note that the bounding set $\mathbb{E}_{t+k|t}$ of the estimation error ε_{t+k} can be precomputed at time t for all $t \in \mathbb{N}$ and all $k \in \mathbb{N}$, regardless of the actual subsequent disturbances and control actions in the next k steps. The precomputation of the bounds for the estimation error enables us to robustly plan the control actions over the prediction horizon. We now establish the time-invariant bounding set \mathbb{E}_∞ of the estimation error in steady state by the following corollary, which will be used to bound the control error (Section III-B).

Corollary III.1. *In steady state, it is guaranteed that the estimation error $\varepsilon_t \in \mathbb{E}_\infty := \{\varepsilon \mid \varepsilon^\top P_\infty^{-1} \varepsilon \leq 1\}$, where P_∞ is the steady-state solution of the equation (7).*

Proof. Similar to the proof of Proposition III.1, from the equation (6) and the definition of the estimation error, we have $\varepsilon_t^\top P_{t|t}^{-1} \varepsilon_t \leq 1 - \delta_t^2$ for all $t \in \mathbb{N}$. In steady state, we have $\varepsilon_t^\top P_\infty^{-1} \varepsilon_t \leq 1 - \delta_t^2 \leq 1$ by the fact that $\delta_t^2 \geq 0, \forall t \in \mathbb{N}$. ■

Note that the time-invariant bounding ellipsoid \mathbb{E}_∞ is also precomputable. We now present our method of computing bounds for the control error.

B. Bounding the Control Error

We consider a control law combining a feed-forward component, given by the tube-based model predictive controller, and a feedback component [6], [9]:

$$u_t(\hat{x}_t) = c_t + K(\hat{x}_t - s_t), \quad (10)$$

where $K \in \mathbb{R}^{m \times n}$ is a fixed feedback matrix satisfying $\rho(A + BK) < 1$. With this control law, we can decouple

¹Detailed proof is provided in Appendix A.

the system dynamics (1) into a nominal state s_t and an error state $e_t := x_t - s_t$. Note that $\hat{x}_t - s_t = e_t + \varepsilon_t$. Thus, the nominal and error state evolve, respectively, according to:

$$s_{t+1} = As_t + Bc_t, \quad s_0 = \hat{x}_0 \quad (11)$$

$$e_{t+1} = A_K e_t + Dw_t + BK\varepsilon_t, \quad e_0 = -\varepsilon_0, \quad (12)$$

where $A_K := A + BK$. Above, the nominal state s_t is deterministic, and the disturbances only affect the error state e_t . Note that by definition $x_t = s_t + e_t$. Providing we can bound e_t , we can plan the nominal control sequence \mathbf{c} so that the actual state and control satisfy the original constraint (2).

As a comparison of the methods for bounding x_t , the previous work in robust output feedback model predictive control [6], [9] first bounds the state estimate from the nominal state, and then bound the actual state from the state estimate. Our formulation does not suffer from the over-approximation introduced by such hierarchical structure in practice, thus leading to a less conservative robust controller.

By substituting (11) and (12) into (2), the original constraint on the actual state can be reformulated in terms of the nominal and error state:

$$Fs_t + Gc_t + (F + GK)e_t + GK\varepsilon_t \leq f. \quad (13)$$

The estimation error ε_t has been bounded in Section III-A. Before computing bounds for the other uncertain state e_t , we make the following steady state assumption:

Assumption III.1. *The recursive state estimation (6)–(9) achieves its steady state before control is applied.*

The above assumption is a common setting in robust model predictive control [6]–[8], [24]. In practice, the steady-state operation of the estimation module before applying the actual control is also desirable and achievable. For example, motion capture systems or onboard sensors on robots are usually turned on before the control module for a long enough time to reach a better estimation accuracy. Hereafter, the time indices of variables are defined with respect to the start of control, and that the matrix $P_{t+k|t+k}$ in Proposition III.1 shall be replaced with P_∞ .

We recall the following standard definition of (robust) positively invariant set [25], [26]:

Definition III.1. A set $\Omega \subset \mathbb{R}^n$ is said *positively invariant* for the system $x_{t+1} = f(x_t)$ if $f(x_t) \in \Omega$ for all $x_t \in \Omega$. A set $\Omega \subset \mathbb{R}^n$ is said *robust positively invariant* for the system $x_{t+1} = f(x_t, w_t)$ and the constraint set \mathbb{W} if $f(x_t, w_t) \in \Omega$ for all $x_t \in \Omega$ and all $w_t \in \mathbb{W}$.

The error state dynamics (12) can be rewritten in the form:

$$e_{t+1} = A_K e_t + \vartheta_t, \quad \vartheta_t := Dw_t + BK\varepsilon_t, \quad (14)$$

where ϑ_t lies in the C set Θ defined by:

$$\Theta := D\mathbb{W} \oplus BK\mathbb{E}_\infty \quad (15)$$

by the fact that $\varepsilon_t \in \mathbb{E}_\infty$ for all $t \in \mathbb{N}$ from Assumption III.1 and Corollary III.1. Since $\rho(A_K) < 1$, there exists a C set \mathbb{S} that is finite time computable and robust positively invariant for the system (14) and the constraint set Θ [26]. We refer

to [27, Chapter 3] for details on computing robust positively invariant sets. The following proposition bounds the error state e_t into the future:

Proposition III.2. *If the initial system and nominal state, x_0 and s_0 , respectively, satisfy $e_0 = x_0 - s_0 \in \mathbb{S}$, then $e_t \in \mathbb{S}$ for all $t \in \mathbb{N}$, and all admissible disturbance sequences \mathbf{w} and \mathbf{v} .*

Proof. Follows immediately from the definition of robust positively invariant sets in Definition III.1. ■

In practice, we choose $s_0 = \hat{x}_0$. Thus, the initial condition of Proposition III.2 is equivalent to $-\varepsilon_0 \in \mathbb{S}$. Note that $\varepsilon_0 \in \mathbb{E}_{0|0}$ and that $\mathbb{E}_{0|0}$ is symmetric about the origin. The initial condition is then guaranteed to be satisfied if $\mathbb{E}_{0|0} \subset \mathbb{S}$. In contrast, the initial condition of the estimation error in the previous work [6] is a pure assumption, the satisfaction of which cannot be checked at the time of control.

With the two uncertain states e_t and ε_t bounded in the constraint (13), we are now ready to design the robust model predictive controller.

IV. ROBUST MPC WITH STATE ESTIMATION

In this section, we present three different robust model predictive controllers with set-membership (SM) state estimation, whose properties may be desirable for different systems. With the previously described propositions on bounds for the uncertain states, we can guarantee the satisfaction of the original constraint (2) by planning the nominal state under tighter constraints. Let $s_{t+k|t}$ be the predicted nominal state and $c_{t+k|t}^*$ be the optimal nominal control action into the future at time t . The three different approaches adopt different choices of $s_{t|t}$ when solving the optimal control problem at time t , and the differences are summarized as:

- 1) *Safe SM-MPC:* The nominal state $s_{t|t}$ is chosen to be s_t , which evolves according to the dynamics (11), i.e., $s_{t+1} = As_t + Bc_{t|t}^*$, $s_0 = \hat{x}_0$. The Safe SM-MPC guarantees recursive feasibility and stability and generalizes well to high-dimensional systems, but the closed-loop behavior is relatively more conservative than the following two controllers (still less conservative than the previous work [6]).
- 2) *Aggressive SM-MPC:* The nominal state $s_{t|t}$ is an optimization variable to be decided. The resulting controller exhibits less conservative behavior than the Safe SM-MPC, but lacks guarantees for feasibility and stability.
- 3) *Switching SM-MPC:* This approach switches between the above two controllers. The Switching SM-MPC inherits the recursive feasibility and stability from the Safe SM-MPC and less conservative closed-loop behavior from the Aggressive SM-MPC, but suffers from computational complexity of high-dimensional problems.

Note that the nominal state $s_{t+k|t}$ in all the above three approaches evolves according to the dynamics (11) within the prediction horizon of the optimal control problem at time t , i.e., $s_{t+k+1|t} = As_{t+k|t} + Bc_{t+k|t}^*$ with $s_{t|t}$ as the initial value.

A. Controller Design for Safe SM-MPC

Note that the original constraint (2) is guaranteed to be satisfied if the inequality (13) holds for all admissible error states e_t and estimation errors ε_t . As a result, the Safe SM-MPC solves the following finite horizon constrained optimal control problem at each time t :

$$\begin{aligned}
V_N^*(s_t) &= \min_{\mathbf{c}_{[t:t+N-1]|t}} \sum_{k=0}^{N-1} q(s_{t+k|t}, c_{t+k|t}) + p(s_{t+N|t}) \\
\text{s.t. } s_{t+k+1|t} &= A s_{t+k|t} + B c_{t+k|t} \\
F s_{t+k|t} + G c_{t+k|t} &\leq f - (F + GK)e_{t+k} - GK\varepsilon_{t+k}, \\
&\quad \forall e_{t+k} \in \mathbb{S}, \quad \forall \varepsilon_{t+k} \in \mathbb{E}_{t+k|t}, \\
s_{t|t} &= s_t, \quad s_{t+N|t} \in \mathcal{S}_f, \\
k &= 0, 1, \dots, N-1,
\end{aligned} \tag{16}$$

where $\mathbf{c}_{[t:t+N-1]|t} := \{c_{t|t}, c_{t+1|t}, \dots, c_{t+N-1|t}\}$ is the control sequence, s_t is the closed-loop nominal state evolving according to $s_{t+1} = A s_t + B c_{t|t}^*$ with the initial condition $s_0 = \hat{x}_0$, N is the prediction horizon, $p(\cdot)$ is the terminal cost function, \mathcal{S}_f is the terminal constraint set, \mathbb{S} is the robust positively invariant set for the error state, and $\mathbb{E}_{t+k|t}$ is the bounding set for the estimation error at time $t+k$ given the information available at time t . Note that the computation of $\max_{e_{t+k} \in \mathbb{S}} (F + GK)e_{t+k}$ does not require the expensive Minkowski sum², thus making the algorithm generalize better to high-dimensional systems than the previous work [6], [9].

Let \bar{f} be the tightened constraint considering the error state e_t and the estimation error ε_t , i.e., $\bar{f} := f - \max_{e \in \mathbb{S}} (F + GK)e - \max_{\varepsilon \in \mathbb{E}_\infty} GK\varepsilon$. The positive definite terminal cost $p(\cdot)$ and the terminal constraint set \mathcal{S}_f satisfy the usual stabilizing conditions [28], [29]:

Assumption IV.1. $A_K s \in \mathcal{S}_f$, $(F + GK)s \leq \bar{f}$, $\forall s \in \mathcal{S}_f$.

Assumption IV.2. $p(A_K s) - p(s) \leq -q(s, Ks)$, $\forall s \in \mathcal{S}_f$.

The choices of the terminal cost and the terminal constraint set satisfying the above conditions are the same as those in the nominal MPC with the only difference in using the tightened constraint \bar{f} rather than the original constraint f .

Upon solving (16) at time t , the controller applies

$$u_t(\hat{x}_t) = c_{t|t}^* + K(\hat{x}_t - s_t) \tag{17}$$

to the system, where \hat{x}_t is the state estimate given by (8), and $c_{t|t}^*$ is the first element in the optimal nominal control sequence from (16). The controller (17) along with the state estimation (8) forms the receding horizon control strategy for the system.

We summarize the control procedure in Algorithm 1. Note that step 5 requires only one optimization for $k=0$, the results for the other k values can be scaled from the case of $k=0$ based on the value of β and ρ . In addition, step 5 can be precomputed before control if we relax the bounding set $\mathbb{E}_{t+k|t}$ to \mathbb{E}_∞ , which leads to computing $\max_{\varepsilon \in \mathbb{E}_\infty} GK\varepsilon$.

²Detailed explanation is provided in Appendix B.

Algorithm 1 Safe SM-MPC

Require: State estimation parameters $\beta, \rho \in (0, 1)$, Stabilizing feedback matrix K , Prediction horizon N

- 1: **Initialize** the nominal state $s_0 \leftarrow \hat{x}_0$
- 2: Compute $\max_{e \in \mathbb{S}} (F + GK)e$ and $\max_{\varepsilon \in \mathbb{E}_\infty} GK\varepsilon$ to obtain the tightened constraint \bar{f}
- 3: Compute the constraint set \mathcal{S}_f and the terminal cost $p(\cdot)$
- 4: **repeat** at each time $t = 0, 1, 2, \dots$
- 5: Compute $\max_{\varepsilon_{t+k} \in \mathbb{E}_{t+k|t}} GK\varepsilon_{t+k}$, $k = 0, \dots, N-1$
- 6: Obtain the state estimate \hat{x}_t from (8)
- 7: Solve problem (16) to obtain $c_{t|t}^*$
- 8: Apply $u_t = c_{t|t}^* + K(\hat{x}_t - s_t)$ to the system
- 9: $s_{t+1} \leftarrow A s_t + B c_{t|t}^*$
- 10: **until** convergence

We now establish the recursive feasibility and stability of Safe SM-MPC:

Theorem IV.1. Consider system (1) controlled by the Safe SM-MPC controller (16) and (17). Suppose that problem (16) is feasible at time $t = 0$, then the Safe SM-MPC controller (16) and (17) is feasible for all $t \geq 0$. Moreover, the set \mathbb{S} is robustly asymptotically stable for the closed-loop system (1), (16) and (17).

Proof. The proof follows from standard MPC arguments. Assume that at time t the optimal control problem (16) is feasible and let $\{s_{t|t}^*, s_{t+1|t}^*, \dots, s_{t+N-1|t}^*, s_{t+N|t}^*\}$ and $\{c_{t|t}^*, c_{t+1|t}^*, \dots, c_{t+N-1|t}^*\}$ be the optimal nominal trajectory and control sequence. At time $t+1$, we have:

$$s_{t+1} = A s_t + B c_{t|t}^* = A s_{t|t}^* + B c_{t|t}^* = s_{t+1|t}^*.$$

In addition, by the fact that $\delta_{t+1}^2 \geq (1-\beta)(1-\rho)\delta_t^2$ and Proposition III.1, we know that

$$\mathbb{E}_{t+1+k|t+1} \subset \mathbb{E}_{t+1+k|t} \subset \mathbb{E}_\infty, \quad \forall k \in \mathbb{N}. \tag{18}$$

Thus, the nominal state trajectory

$$\{s_{t+1|t}^*, s_{t+2|t}^*, \dots, s_{t+N-1|t}^*, s_{t+N|t}^*, A_K s_{t+N|t}^*\} \tag{19}$$

and the related control sequence

$$\{c_{t+1|t}^*, c_{t+2|t}^*, \dots, c_{t+N-1|t}^*, K s_{t+N|t}^*\} \tag{20}$$

is a feasible solution to the problem (16) at time $t+1$ by Assumption IV.1 and the fact that $s_{t+N|t}^* \in \mathcal{S}_f$. Therefore, we conclude by induction that the Safe SM-MPC controller (16) and (17) is feasible $\forall t \geq 0$.

We next show that $V_N^*(\cdot)$ is decreasing along the trajectory. Note that (19) and (20) is a suboptimal solution to the problem (16) at time $t+1$, therefore we have:

$$\begin{aligned}
V_N^*(s_{t+1}) &\leq \sum_{k=1}^{N-1} q(s_{t+k|t}^*, c_{t+k|t}^*) \\
&\quad + q(s_{t+N|t}^*, K s_{t+N|t}^*) + p(A_K s_{t+N|t}^*) \\
&= V_N^*(s_t) - q(s_{t|t}^*, c_{t|t}^*) - p(s_{t+N|t}^*) \\
&\quad + q(s_{t+N|t}^*, K s_{t+N|t}^*) + p(A_K s_{t+N|t}^*).
\end{aligned}$$

Therefore we have:

$$V_N^*(s_{t+1}) - V_N^*(s_t) \leq -q(s_{t|t}^*, c_{t|t}^*)$$

by Assumption IV.2 and the fact that $s_{t+N|t}^* \in \mathcal{S}_f$. Note that the stage cost $q(\cdot)$ and the terminal cost $p(\cdot)$ are both positive definite. Therefore, the optimal cost $V_N^*(\cdot)$ is a decreasing Lyapunov function along the closed-loop trajectory, which implies that the nominal state s_t converges to the origin as $t \rightarrow \infty$. Moreover, we know that $x_t \in s_t \oplus \mathbb{S}$ by the definition of the error state. Thus, we conclude that the set \mathbb{S} is asymptotically stable for the closed-loop system. ■

B. Controller Design for Aggressive SM-MPC

The Aggressive SM-MPC is inspired by some existing methods [6], [9], [10], where the nominal state $s_{t|t}$ is also a decision variable as the nominal control sequence at time t . The finite horizon constrained optimal control problem solved online is:

$$\begin{aligned} V_N^*(\hat{x}_t) &= \min_{s_{t|t}, c_{[t:t+N-1]|t}} \sum_{k=0}^{N-1} q(s_{t+k|t}, c_{t+k|t}) + p(s_{t+N|t}) \\ \text{s.t. } & s_{t+k+1|t} = A s_{t+k|t} + B c_{t+k|t} \\ & F s_{t+k|t} + G c_{t+k|t} \leq f - (F + GK)e_{t+k} - GK\varepsilon_{t+k}, \\ & \quad \forall e_{t+k} \in \mathbb{S}, \quad \forall \varepsilon_{t+k} \in \mathbb{E}_{t+k|t}, \\ & \hat{x}_t - s_{t|t} \in \mathbb{S} \ominus \mathbb{E}_{t|t}, \quad s_{t+N|t} \in \mathcal{S}_f, \\ & k = 0, 1, \dots, N-1. \end{aligned} \quad (21)$$

The only difference between the problem (16) and (21) is the choice of the *initial* nominal state $s_{t|t}$ within the prediction horizon at each time t . The constraint of $\hat{x}_t - s_{t|t} \in \mathbb{S} \ominus \mathbb{E}_{t|t}$ ensures that $e_{t+k} \in \mathbb{S}$ over the prediction horizon. The resulting control procedure is the same as Algorithm 1 with the replacement of problem (16) by problem (21) in step 7 and the removal of step 9. With one more degree of freedom in the optimization problem, the Aggressive SM-MPC shows less conservative closed-loop behavior compared to the Safe SM-MPC. However, the feasibility of problem (21) at time t does not imply the feasibility at time $t+1$, which also makes the stability property not guaranteed. Moreover, the extra condition on $s_{t|t}$ requires the explicit computation of the robust positively invariant set \mathbb{S} using Minkowski sum, whose computational complexity may prevent the application of the Aggressive SM-MPC on high-dimensional systems.

C. Controller Design for Switching SM-MPC

The Switching SM-MPC always saves the closed-loop nominal state s_t as a feasible solution for $s_{t|t}$ at time $t-1$, while trying to optimize over $s_{t|t}$ by solving problem (21) whenever feasible. To maintain the stability of the controller, we check the decreasing condition on $V_N^*(\cdot)$ online at each time t . The resulting control procedure is summarized in Algorithm 2.

The following theorem establishes the recursive feasibility and stability of the Switching SM-MPC in Algorithm 2:

Algorithm 2 Switching SM-MPC

Require: $\beta, \rho \in (0, 1)$, K , N

- 1: **Initialize:** $s_0 \leftarrow \hat{x}_0$, $V_{\text{prev}} \leftarrow +\infty$
 - 2: Compute the tightened constraint \bar{f}
 - 3: Compute the constraint set \mathcal{S}_f and the terminal cost $p(\cdot)$
 - 4: **repeat** at each time $t = 0, 1, 2, \dots$
 - 5: Compute $\max_{\varepsilon_{t+k} \in \mathbb{E}_{t+k|t}} GK\varepsilon_{t+k}$, $k = 0, \dots, N-1$
 - 6: Obtain the state estimate \hat{x}_t from (8)
 - 7: **try**
 - 8: Solve problem (21) to obtain $s_{t|t}^*$, $c_{t|t}^*$, and V_N^*
 - 9: **if** $V_N^* < V_{\text{prev}}$ **then** $V_{\text{prev}} \leftarrow V_N^*$, $s_t \leftarrow s_{t|t}^*$
 - 10: **else raise** Exception
 - 11: **end if**
 - 12: **except**
 - 13: Solve problem (16) to obtain $c_{t|t}^*$
 - 14: **end try**
 - 15: Apply $u_t = c_{t|t}^* + K(\hat{x}_t - s_t)$ to the system
 - 16: $s_{t+1} \leftarrow A s_t + B c_{t|t}^*$
 - 17: **until** convergence
-

Theorem IV.2. Consider system (1) controlled by the Switching SM-MPC in Algorithm 2. Suppose that either problem (16) or (21) is feasible at time $t = 0$, then the Switching SM-MPC controller in Algorithm 2 is feasible for all $t \geq 0$. Moreover, the set \mathbb{S} is robustly asymptotically stable for the closed-loop system.

Proof. Detailed proof is provided in Appendix C. ■

V. SIMULATION EXAMPLES

We evaluate the proposed controllers on three different applications: double integrator, robotic walker, and quadrotor. A comparison with LQR [30], nominal MPC, and robust output feedback MPC [6] is also provided. The code will be released upon publication. Hereafter, we refer to the classical results shown in [6] as Mayne's MPC for brevity. In the following subsections, the stage cost and terminal cost are defined by:

$$q(s, c) := (1/2)[s^\top \tilde{Q}s + c^\top \tilde{R}c], \quad p(s) := (1/2)s^\top \tilde{P}s,$$

where \tilde{P} , \tilde{Q} and \tilde{R} are positive definite matrices.

A. Double Integrator

We use the same example as in Mayne's MPC paper to compare the performance of our controllers and the baselines. The model is a double integrator of the form:

$$x_{t+1} = \begin{bmatrix} 1 & 1 \\ 0 & 1 \end{bmatrix} x_t + \begin{bmatrix} 1 \\ 1 \end{bmatrix} u_t + w_t, \quad y_t = [1 \quad 1] x_t + v_t,$$

with additive disturbances $(w_t, v_t) \in \mathbb{W} \times \mathbb{V}$ where $\mathbb{W} := \{w \in \mathbb{R}^2 \mid \|w\|_2 \leq \sqrt{2}\lambda, \lambda \in \mathbb{R}_+\}$ and $\mathbb{V} := \{v \in \mathbb{R} \mid |v| \leq \mu, \mu \in \mathbb{R}_+\}$. The state and control constraints are $(x_t, u_t) \in \mathbb{X} \times \mathbb{U}$ where $\mathbb{X} := \{x \in \mathbb{R}^2 \mid x_1 \in [-50, 3], x_2 \in [-50, 3]\}$ and $\mathbb{U} := \{u \in \mathbb{R} \mid |u| \leq 3\}$. The weighting matrices in the stage cost are $\tilde{Q} = I$ and $\tilde{R} = 0.01$; the matrix \tilde{P} in the terminal cost is the solution to the algebraic Riccati equation

TABLE I: Closed-loop performance of different controllers for double integrator with $\mu = 0.05$

Method	$\lambda = 0.05$			$\lambda = 0.10$			$\lambda = 0.15$			$\lambda = 0.20$		
	# infeas.	# steps	min D2C	# infeas.	# steps	min D2C	# infeas.	# steps	min D2C	# infeas.	# steps	min D2C
Nominal MPC	72	11.50	0.006	76	10.42	0.010	81	10.21	0.069	81	9.74	0.097
Mayne's MPC	0	16.22	0.588	0	14.19	0.882	100	-	-	100	-	-
Safe SM-MPC	0	12.91	0.308	0	12.67	0.443	0	13.60	0.567	0	15.63	0.721
Aggressive SM-MPC	0	12.23	0.256	3	11.67	0.376	13	11.84	0.490	13	12.29	0.590
Switching SM-MPC	0	12.06	0.250	0	11.67	0.378	0	11.69	0.471	0	12.35	0.599

TABLE II: Closed-loop performance of different controllers for double integrator with $\lambda = 0.10$

Method	$\mu = 0.05$			$\mu = 0.10$			$\mu = 0.15$			$\mu = 0.20$		
	# infeas.	# steps	min D2C	# infeas.	# steps	min D2C	# infeas.	# steps	min D2C	# infeas.	# steps	min D2C
Nominal MPC	76	10.42	0.378	100	-	-	100	-	-	100	-	-
Mayne's MPC	0	14.19	0.882	100	-	-	100	-	-	100	-	-
Safe SM-MPC	0	12.67	0.443	0	14.51	0.580	0	14.77	0.640	0	16.17	0.703
Aggressive SM-MPC	3	11.67	0.376	1	12.69	0.499	3	12.76	0.557	6	13.28	0.667
Switching SM-MPC	0	11.67	0.378	0	12.80	0.472	0	12.62	0.546	0	13.34	0.643

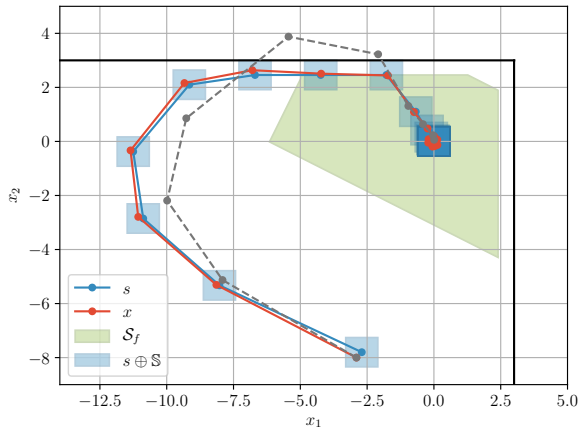


Fig. 2: Closed-loop response of the double integrator. The unknown state trajectory x_t is bounded by the tube $\{s_t \oplus \mathbb{S}\}$ generated by the proposed controller. The dashed line represents the state trajectory generated by the nominal MPC without the state constraints.

of the unconstrained optimal control problem for the nominal system; the feedback control matrix K is the associated LQR controller; the output injection matrix L used in Mayne's MPC is set to be the same as in the original paper [6]. The terminal constraint set \mathcal{S}_f is the maximal positively invariant set [25] for system $s_{t+1} = (A + BK)s$ under the tighter constraint \bar{f} . The prediction horizon is $N = 15$. The optimal state estimation parameters β and ρ are determined offline by a grid search such that the trace of the matrix P_∞ is minimized.

Figure 2 shows the closed-loop trajectory generated by the Safe SM-MPC, for an initial state $x_0 \in s_0 \oplus \mathbb{S}$ where $s_0 = (-2.7, -7.8)^\top$ and a random sequence of admissible state and output disturbances with $\lambda = 0.1$ and $\mu = 0.05$.³ As shown by the dashed line in Figure 2, MPC can achieve faster convergence rate by making use of the space. In this example, the closer the controller gets to the constraint of $x_2 \leq 3$, the less conservative the closed-loop system is.

³The tube shown in Figure 2 is the minimum bounding box for the true set $\{s_t \oplus \mathbb{S}\}$, as the exact shape of \mathbb{S} cannot be explicitly computed for the ellipsoidal uncertainty sets.

For each combination of λ and μ , we compare different methods over 100 runs with different realizations of admissible state and output disturbances. The performance is evaluated by the following three metrics:

- 1) # infeas.: the *total* number of infeasibility that occurs;
- 2) # steps: the *average* number of steps to convergence;
- 3) min D2C: the *average minimum Distance* from the closed-loop state **to** the **Constraint** of $x_2 \leq 3$.

The last two metrics are only computed over runs without the loss of feasibility. The initial state $x_0 = (-3.1, -8)^\top$ and the convergence to the origin is declared once the norm of \hat{x}_t is less than $\max(\lambda, \mu)$. The common parameters across all methods are set to be the same. Here, LQR fails to satisfy the constraint for every single run, leading to the # infeas. being 100, thus is omitted in the comparison.

Table I and Table II summarize the results. As shown, the Aggressive SM-MPC and Switching SM-MPC generate the least conservative closed-loop behaviors, and the feasibility of the Safe SM-MPC and Switching SM-MPC is preserved over the full range of disturbances. By contrast, the nominal MPC fails due to the ignorance of disturbances in the model and the infeasibility of Mayne's MPC comes from the conservatively tightened constraints under larger uncertainties. Note that the Safe SM-MPC also exhibits less conservative closed-loop behavior than Mayne's MPC.

B. Robotic Walker

We further validate our approach on a robotic walker [31], which can be modeled as a two-wheeled inverted pendulum with state $x = [r, \dot{r}, \theta, \dot{\theta}, \psi, \dot{\psi}]^\top \in \mathbb{R}^6$ where r is the linear displacement, θ is the pitch angle, and ψ is the yaw angle. The inputs to the system, $u = [T_\theta, T_\psi]^\top \in \mathbb{R}^2$, are the torques around the lateral and vertical axis respectively. We assume that the matrix D in (1) is an identity matrix and the state disturbance lives in the bounding ellipsoid of the hyperrectangle defined by the points $[\pm 0.01, \pm 0.02, \pm \pi/600, \pm 0.01, \pm \pi/600, \pm 0.02]^\top$. The output matrix C is defined as an identity matrix as in [31], and the output disturbance lives in the axis-aligned bound-

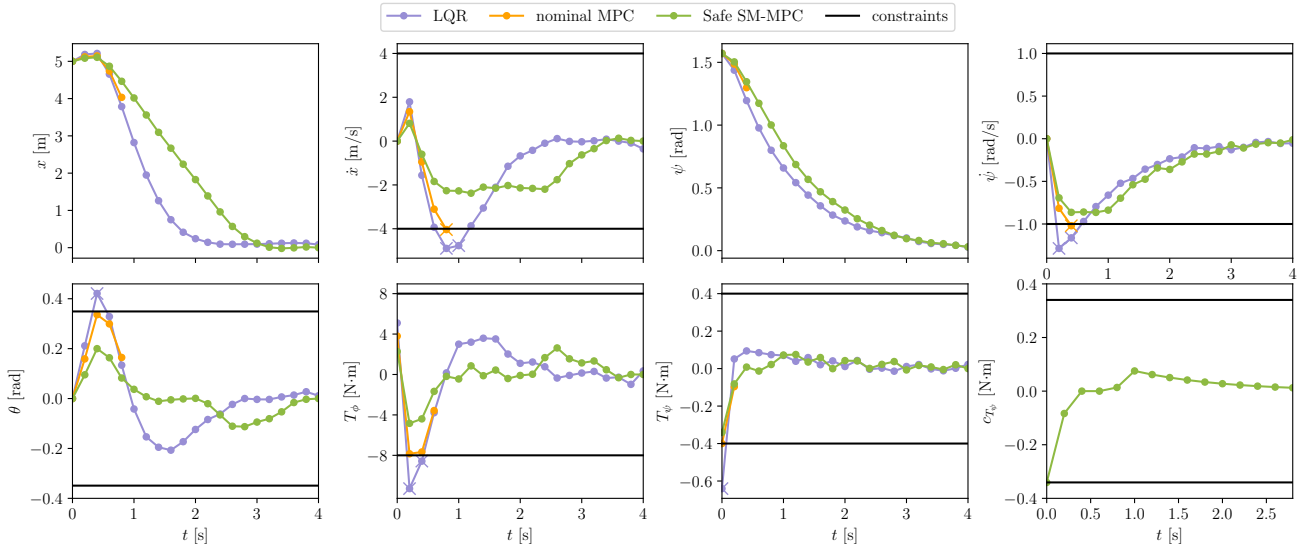


Fig. 3: Closed-loop response of the robotic walker system. The left four figures correspond to the subsystem (i) and the right four figures correspond to the subsystem (ii). The cross over the points indicates the occurrence of infeasibility. The incomplete trajectory of the nominal MPC results from the failure of the optimization solver after an infeasible problem is detected. The last figure on the bottom right shows the planned nominal control action at time $t = 0$ under tightened constraint for the rotation subsystem about the vertical axis.

ing ellipsoid of the hyperrectangle formed by the points $[\pm 0.02, \pm 0.02, \pm \pi/600, \pm 0.01, \pm \pi/360, \pm 0.02]^\top$. The control task is to regulate the robot from the initial state $x_0 = [5, 0, 0, 0, \pi/2, 0]^\top$ to the origin while satisfying the constraint of $(x, u) \in \mathbb{X} \times \mathbb{U}$ where $\mathbb{X} := \{x \in \mathbb{R}^6 \mid |\dot{r}| \leq 4, |\theta| \leq \pi/9, |\psi| \leq 1\}$ and $\mathbb{U} := \{u \in \mathbb{R}^2 \mid |T_\theta| \leq 8, |T_\psi| \leq 0.4\}$.

The robotic walker model can be decoupled into two separate subsystems: (i) a pendulum system describing the linear displacement and rotation about the lateral axis and (ii) a rotation system describing the rotation about the vertical axis [32]. We apply controllers with identical common parameters to the two subsystems independently.

Figure 3 summarizes the results. As shown, the Safe SM-MPC robustly drives the system towards the origin under disturbances. LQR fails due to unmodeled constraints while the nominal MPC fails due to unmodeled disturbances. Mayne’s MPC, Aggressive SM-MPC and Switching SM-MPC fail to solve the optimal control problem in this example due to the expensive Minkowski sum in the computation of the robust positively invariant set.

C. Quadrotor Dynamics

Finally to validate our approach scales well to high-dimensional systems, we apply the proposed controller to a quadrotor model with state $x = [\mathbf{p}, \mathbf{R}, \mathbf{v}, \boldsymbol{\Omega}]^\top \in \mathbb{R}^{12}$ where $\mathbf{p} = [p_x, p_y, p_z]$ is the position, $\mathbf{R} = [\phi, \theta, \psi]$ is the orientation, $\mathbf{v} = [v_x, v_y, v_z]$ is the translational velocity, and $\boldsymbol{\Omega} = [\omega_\phi, \omega_\theta, \omega_\psi]$ is the angular velocity [33], [34]. The inputs to the model, $u = [T, M_x, M_y, M_z]^\top \in \mathbb{R}^4$, are the total thrust and moment respectively. Detailed description of disturbances, state and input constraint, and the linearized model around the equilibrium state are provided in Appendix D. The regulation task is to drive the system from the initial state of $\mathbf{p} = [5, 4, 0]^\top$, $\mathbf{R} = [0, 0, 0]^\top$, $\mathbf{v} = [0, 0, 0]^\top$, $\boldsymbol{\Omega} = [0, 0, 0]^\top$ to the origin.

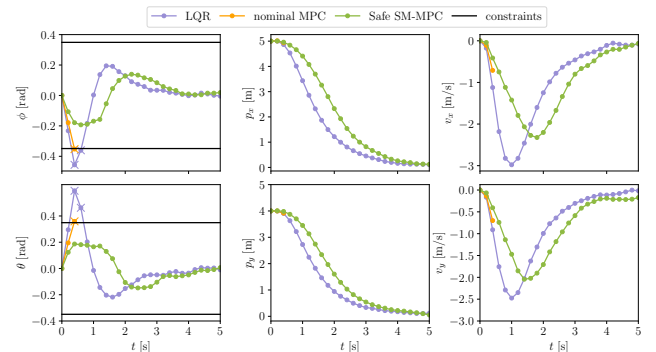


Fig. 4: Closed-loop response of the quadrotor system.

Figure 4 shows part of the results. As in the robotic walker example, the Safe SM-MPC is the only controller that robustly drives the system to the origin while maintaining recursive feasibility and stability of the closed-loop system.

VI. CONCLUSION

In conclusion, we presented a set of novel approaches for robust output feedback model predictive control of constrained linear systems in the presence of bounded state and output disturbances. Considering the nature of real-world disturbances and the requirement for low computational complexity, we adopt ellipsoidal set-membership state estimation which describes the uncertainty set of disturbances as ellipsoids rather than boxes or polytopes. The proposed controllers were evaluated in simulation on three different systems and were shown to improve closed-loop performance beyond baseline methods while ensuring robust constraint satisfaction, recursive feasibility and stability. Due to the construction of feasible nominal states, the Safe SM-MPC does not require explicit computation of robust positively invariant set, thus scaling well to high-dimensional systems.

A. Lemma for Proposition III.1

Lemma. *The matrix $[(1-\rho)^{-1}CP_{t+k+1|t+k}C^\top + \rho^{-1}R]^{-1}$ is positive definite.*

Proof. Note that $0 < \beta < 1$ and that the matrix Q and $P_{t|t}$ are both positive definite [16]. From (7), for all $t \in \mathbb{N}$ and all $z \in \mathbb{R}^n$, we have:

$$z^\top P_{t+1|t}z = (1-\beta)^{-1}(z^\top A)P_{t|t}(A^\top z) + \beta^{-1}(z^\top D)Q(D^\top z) \geq 0.$$

Thus for all $t \in \mathbb{N}$, all $k \in \mathbb{N}$, and all $z \in \mathbb{R}^n \setminus \{0\}$, we have:

$$(1-\rho)^{-1}(z^\top C)P_{t+k+1|t+k}(C^\top z) + \rho^{-1}z^\top Rz > 0$$

by the fact that R is positive definite and that $0 < \rho < 1$. Therefore the matrix $[(1-\rho)^{-1}CP_{t+k+1|t+k}C^\top + \rho^{-1}R]$ is positive definite. It is known that the inverse of a positive definite matrix is also positive definite. Thus we conclude that the matrix $[(1-\rho)^{-1}CP_{t+k+1|t+k}C^\top + \rho^{-1}R]^{-1}$ is positive definite, which gives the lemma. ■

B. Note for the Computation of Constraint Tightening

In this subsection, we provide implementation details on computing $\max_{e \in \mathbb{S}}(F + GK)e$. The proposed algorithm is an extension of the method in [27, Chapter 3] to ellipsoidal uncertainty sets.

Let a pair of positive integers r_1, r_2 and a pair of scalars $0 \leq \alpha_1, \alpha_2 < 1$ satisfy:

$$A_K^{r_1}D\mathbb{W} \subset \alpha_1 D\mathbb{W}, \quad A_K^{r_2}BK\mathbb{E}_\infty \subset \alpha_2 BK\mathbb{E}_\infty. \quad (22)$$

It can be shown that the minimal robust positively invariant set approximation for e_t can be determined as [27, Chapter 3]:

$$\mathbb{S} \doteq \frac{1}{1-\alpha_1} \bigoplus_{j=0}^{r_1-1} A_K^j D\mathbb{W} \oplus \frac{1}{1-\alpha_2} \bigoplus_{j=0}^{r_2-1} A_K^j BK\mathbb{E}_\infty.$$

Therefore, we have:

$$\begin{aligned} \max_{e \in \mathbb{S}}(F + GK)e &= \frac{1}{1-\alpha_1} \sum_{j=0}^{r_1-1} \max_{w_j \in \mathbb{W}} (F + GK)A_K^j D w_j \\ &\quad + \frac{1}{1-\alpha_2} \sum_{j=0}^{r_2-1} \max_{\varepsilon_j \in \mathbb{E}_\infty} (F + GK)A_K^j BK \varepsilon_j, \end{aligned}$$

which is a convex optimization problem. In cases where D is full row rank, we know that $A_K^{r_1}D\mathbb{W} \subset \alpha_1 D\mathbb{W}$ if and only if $D^\dagger A_K^{r_1}D\mathbb{W} \subset \alpha_1 \mathbb{W}$, where D^\dagger is the Moore-Penrose pseudoinverse of D . In other words, for all $w \in \mathbb{W}$, the point $D^\dagger A_K^{r_1}Dw$ lies in the scaled ellipsoid $\alpha_1 \mathbb{W}$. The same reasoning applies to cases where $\theta := BK$ is full row rank. Therefore, the condition (22) is equivalent to:

$$\max_{w \in \mathbb{W}} (D^\dagger A_K^{r_1}Dw)^\top Q^{-1} (D^\dagger A_K^{r_1}Dw) \leq \alpha_1^2, \quad (23)$$

$$\max_{\varepsilon \in \mathbb{E}_\infty} (\theta^\dagger A_K^{r_2} \theta \varepsilon)^\top P_\infty^{-1} (\theta^\dagger A_K^{r_2} \theta \varepsilon) \leq \alpha_2^2. \quad (24)$$

Given r_1, r_2 , the optimal value of α_1, α_2 can be computed

accordingly. More accurate approximation of the robust positively invariant set can be achieved with larger r_1, r_2 and smaller α_1, α_2 . Although (23) and (24) are non-convex problems, the optimizer [35] always return the optimal solution efficiently in our experiments with non-zero initializations.

In cases where either D or θ are row rank-deficient, one can *either* (i) find a full-dimensional bounding ellipsoid of $D\mathbb{W}$ or $\theta\mathbb{E}_\infty$ and follow the proposed algorithm, *or* (ii) find a full-dimensional bounding polytope of $D\mathbb{W}$ or $\theta\mathbb{E}_\infty$ and follow the standard procedure in [27, Chapter 3]. We note that the computation of $\max_{e \in \mathbb{S}}(F + GK)e$ described in this subsection does not require the expensive Minkowski sum, making the proposed algorithm generalize well to high-dimensional systems.

C. Proof of Theorem IV.2

Proof. Note that if Algorithm 2 solves problem (16) at time t , it is guaranteed that there exists a feasible solution to problem (16) at time $t + 1$ by Theorem IV.1. Therefore, we only have to show that the solution to problem (21) at time t provides a solution to problem (16) at time $t + 1$. Assume that at time t the problem (21) is feasible and let $\{s_{t|t}^*, s_{t+1|t}^*, \dots, s_{t+N-1|t}^*, s_{t+N|t}^*\}$ and $\{c_{t|t}^*, c_{t+1|t}^*, \dots, c_{t+N-1|t}^*\}$ be the optimal nominal trajectory and control sequence. With the same reasoning as in the proof of Theorem IV.1, we can show that the nominal state trajectory

$$\{s_{t+1|t}^*, s_{t+2|t}^*, \dots, s_{t+N-1|t}^*, s_{t+N|t}^*, A_K s_{t+N|t}^*\}$$

and the related control sequence

$$\{c_{t+1|t}^*, c_{t+2|t}^*, \dots, c_{t+N-1|t}^*, K s_{t+N|t}^*\}$$

is a feasible solution for problem (16) at time $t + 1$, which concludes the proof for recursive feasibility.

To prove stability, we only have to show that V_N^* is decreasing in the case where problem (21) is solved at time t and problem (16) is solved at time $t + 1$. Again, with the same reasoning as in the proof of Theorem IV.1, we can show that $V_N^*(s_{t+1}) - V_N^*(\hat{x}_t) \leq -q(s_{t|t}^*, c_{t|t}^*)$, where $V_N^*(s_{t+1})$ comes from problem (16) and $V_N^*(\hat{x}_t)$ from problem (21). The remaining proof is identical to that in Theorem IV.1. ■

D. Details on Quadrotor Dynamics Example

The quadrotor dynamics with 12 states, 4 inputs can be described as:

$$\begin{aligned} \dot{\mathbf{p}} &= \mathbf{v}, & m\dot{\mathbf{v}} &= m\mathbf{g}e_3 - T\mathbf{R}e_3, \\ \dot{\mathbf{R}} &= \mathbf{R}\hat{\boldsymbol{\Omega}}, & J\dot{\boldsymbol{\Omega}} &= \mathbf{M} - \boldsymbol{\Omega} \times J\boldsymbol{\Omega}, \end{aligned} \quad (25)$$

where $\hat{\cdot} : \mathbb{R}^3 \rightarrow SO(3)$ is the hat operator, $m \in \mathbb{R}$ is the mass of the quadrotor, $g \in \mathbb{R}$ is the gravitational force, and $J := \text{diag}(J_x, J_y, J_z)$ is the moment of inertia matrix. The inertial property of the quadrotor model is adopted from [36, Chapter 16]. The model used for control is the linearized model of (25) around the equilibrium state where

$\mathbf{R}_e = [0, 0, 0]^\top$ and $T_e = mg$:

$$\begin{bmatrix} \dot{\mathbf{p}} \\ \dot{\mathbf{R}} \\ \dot{\mathbf{v}} \\ \dot{\boldsymbol{\Omega}} \end{bmatrix} = \begin{bmatrix} \mathbf{0}_{3 \times 3} & \mathbf{0}_{3 \times 3} & \mathbf{I}_3 & \mathbf{0}_{3 \times 3} \\ \mathbf{0}_{3 \times 3} & \mathbf{0}_{3 \times 3} & \mathbf{0}_{3 \times 3} & \mathbf{I}_3 \\ \mathbf{0}_{3 \times 3} & 0 & -g & 0 \\ \mathbf{0}_{3 \times 3} & g & 0 & 0 \\ \mathbf{0}_{3 \times 3} & 0 & 0 & 0 \\ \mathbf{0}_{3 \times 3} & \mathbf{0}_{3 \times 3} & \mathbf{0}_{3 \times 3} & \mathbf{0}_{3 \times 3} \end{bmatrix} \begin{bmatrix} \mathbf{p} \\ \mathbf{R} \\ \mathbf{v} \\ \boldsymbol{\Omega} \end{bmatrix} + \begin{bmatrix} \mathbf{0}_{3 \times 1} & \mathbf{0}_{3 \times 3} \\ \mathbf{0}_{3 \times 1} & \mathbf{0}_{3 \times 3} \\ 0 & \mathbf{0}_{3 \times 3} \\ 0 & \mathbf{0}_{3 \times 3} \\ -1/m & \mathbf{0}_{3 \times 3} \\ \mathbf{0}_{3 \times 1} & \mathbf{J}^{-\top} \end{bmatrix} \begin{bmatrix} \mathbf{T} \\ \mathbf{M} \end{bmatrix}. \quad (26)$$

To apply MPC controllers, a time discretization is used with $dt = 0.2$ s. We assume that the matrix D in (1) is an identity matrix and the state disturbance $w_t \in \mathbb{R}^{12}$ lives in the axis-aligned minimum bounding ellipsoid of the hyperrectangle defined by the points $[\pm 0.01, \pm 0.01, \pm 0.01, \pm \pi/600, \pm \pi/600, \pm \pi/600, \pm 0.02, \pm 0.02, \pm 0.02, \pm 0.01, \pm 0.01, \pm 0.01]^\top$. The output matrix C is defined as an identity matrix as in [34], and the output disturbance lives in the axis-aligned minimum bounding ellipsoid of the hyperrectangle formed by the points $[\pm 0.02, \pm 0.02, \pm 0.02, \pm \pi/600, \pm \pi/600, \pm \pi/600, \pm 0.02, \pm 0.02, \pm 0.02, \pm 0.01, \pm 0.01, \pm 0.01]^\top$. The control task is to regulate the system from the initial state towards the origin while satisfying the constraint of $(x, u) \in \mathbb{X} \times \mathbb{U}$ where $\mathbb{X} := \{x \in \mathbb{R}^{12} \mid |\phi| \leq \pi/9, |\theta| \leq \pi/9, |\psi| \leq \pi/9\}$ and $\mathbb{U} := \{u \in \mathbb{R}^4 \mid |T| \leq 5\}$.

REFERENCES

- [1] A. Bemporad and M. Morari, "Robust model predictive control: A survey," in *Robustness in Identification and Control*. Springer, 1999, pp. 207–226.
- [2] Q. Qiu, F. Yang, Y. Zhu, and E. Mousavinejad, "Output feedback model predictive control based on set-membership state estimation," *IET Control Theory & Applications*, vol. 14, no. 4, pp. 558–567, 2019.
- [3] A. R. de Souza, D. Efimov, T. Raissi, and X. Ping, "Robust output feedback MPC: An interval-observer approach," in *IEEE Conference on Decision and Control (CDC)*, 2020, pp. 2529–2534.
- [4] A. N. Atassi and H. K. Khalil, "A separation principle for the stabilization of a class of nonlinear systems," *IEEE Transactions on Automatic Control*, vol. 44, no. 9, pp. 1672–1687, 1999.
- [5] A. Teel and L. Praly, "Tools for semiglobal stabilization by partial state and output feedback," *SIAM Journal on Control and Optimization*, vol. 33, no. 5, pp. 1443–1488, 1995.
- [6] D. Q. Mayne, S. V. Raković, R. Findeisen, and F. Allgöwer, "Robust output feedback model predictive control of constrained linear systems," *Automatica*, vol. 42, no. 7, pp. 1217–1222, 2006.
- [7] A. Bemporad and A. Garulli, "Output-feedback predictive control of constrained linear systems via set-membership state estimation," *International Journal of Control*, vol. 73, no. 8, pp. 655–665, 2000.
- [8] L. Chisci and G. Zappa, "Feasibility in predictive control of constrained linear systems: the output feedback case," *International Journal of Robust and Nonlinear Control*, vol. 12, no. 5, pp. 465–487, 2002.
- [9] D. Q. Mayne, S. Raković, R. Findeisen, and F. Allgöwer, "Robust output feedback model predictive control of constrained linear systems: Time varying case," *Automatica*, vol. 45, no. 9, pp. 2082–2087, 2009.
- [10] V. T. H. Le, C. Stoica, D. Dumur, T. Alamo, and E. F. Camacho, "Robust tube-based constrained predictive control via zonotopic set-membership estimation," in *IEEE Conference on Decision and Control and European Control Conference*, 2011, pp. 4580–4585.
- [11] "Indoor localization ros wiki," http://wiki.ros.org/indoor_localization, accessed: 2021-09-20.
- [12] P. Du, Z. Huang, T. Liu, T. Ji, K. Xu, Q. Gao, H. Sibai, K. Driggs-Campbell, and S. Mitra, "Online monitoring for safe pedestrian-vehicle interactions," in *IEEE International Conference on Intelligent Transportation Systems (ITSC)*, 2020, pp. 1–8.
- [13] U. Rosolia, X. Zhang, and F. Borrelli, "Robust learning model predictive control for iterative tasks: Learning from experience," in *IEEE Conference on Decision and Control (CDC)*, 2017, pp. 1157–1162.
- [14] Y. Kim, X. Zhang, J. Guanetti, and F. Borrelli, "Robust model predictive control with adjustable uncertainty sets," in *IEEE Conference on Decision and Control (CDC)*, 2018, pp. 5176–5181.
- [15] F. Schweppe, "Recursive state estimation: Unknown but bounded errors and system inputs," *IEEE Transactions on Automatic Control*, vol. 13, no. 1, pp. 22–28, 1968.
- [16] D. Bertsekas and I. Rhodes, "Recursive state estimation for a set-membership description of uncertainty," *IEEE Transactions on Automatic Control*, vol. 16, no. 2, pp. 117–128, 1971.
- [17] L. Chisci, A. Garulli, and G. Zappa, "Recursive state bounding by parallelotopes," *Automatica*, vol. 32, no. 7, pp. 1049–1055, 1996.
- [18] A. Vicino and G. Zappa, "Sequential approximation of feasible parameter sets for identification with set membership uncertainty," *IEEE Transactions on Automatic Control*, vol. 41, no. 6, pp. 774–785, 1996.
- [19] A. Delgado, C. Kambhampati, and K. Warwick, "Dynamic recurrent neural network for system identification and control," *IEEE Proceedings-Control Theory and Applications*, vol. 142, no. 4, pp. 307–314, 1995.
- [20] Y. Wu, A. Isidori, R. Lu, and H. K. Khalil, "Performance recovery of dynamic feedback-linearization methods for multivariable nonlinear systems," *IEEE Transactions on Automatic Control*, vol. 65, no. 4, pp. 1365–1380, 2019.
- [21] J. de Jesús Rubio, "Robust feedback linearization for nonlinear processes control," *ISA Transactions*, vol. 74, pp. 155–164, 2018.
- [22] M. Bujarbaruah, X. Zhang, U. Rosolia, and F. Borrelli, "Adaptive MPC for iterative tasks," in *IEEE Conference on Decision and Control (CDC)*, 2018, pp. 6322–6327.
- [23] D. P. Bertsekas, "Control of uncertain systems with a set-membership description of the uncertainty," Ph.D. dissertation, Massachusetts Institute of Technology, 1971.
- [24] S. Rakovic, "Robust control of constrained discrete time systems: Characterization and implementation," Ph.D. dissertation, University of London, 2005.
- [25] F. Blanchini, "Set invariance in control," *Automatica*, vol. 35, no. 11, pp. 1747–1767, 1999.
- [26] S. V. Rakovic, E. C. Kerrigan, K. I. Kouramas, and D. Q. Mayne, "Invariant approximations of the minimal robust positively invariant set," *IEEE Transactions on Automatic Control*, vol. 50, no. 3, pp. 406–410, 2005.
- [27] B. Kouvaritakis and M. Cannon, *Model predictive control: Classical, robust and stochastic*. Springer, 2015.
- [28] F. Borrelli, A. Bemporad, and M. Morari, *Predictive control for linear and hybrid systems*. Cambridge University Press, 2017.
- [29] D. Q. Mayne, J. B. Rawlings, C. V. Rao, and P. O. Scokaert, "Constrained model predictive control: Stability and optimality," *Automatica*, vol. 36, no. 6, pp. 789–814, 2000.
- [30] D. Liberzon, *Calculus of variations and optimal control theory: a concise introduction*. Princeton university press, 2011.
- [31] A. R. da Silva and F. C. Sup, "A robotic walker based on a two-wheeled inverted pendulum," *Journal of Intelligent & Robotic Systems*, vol. 86, no. 1, pp. 17–34, 2017.
- [32] F. Grasser, A. D'arrigo, S. Colombi, and A. C. Rufer, "JOE: a mobile, inverted pendulum," *IEEE Transactions on Industrial Electronics*, vol. 49, no. 1, pp. 107–114, 2002.
- [33] D. D. Fan, A.-a. Agha-mohammadi, and E. A. Theodorou, "Deep learning tubes for tube MPC," *arXiv preprint arXiv:2002.01587*, 2020.
- [34] P. Liu, J. Geng, Y. Li, Y. Cao, Y. E. Bayiz, J. W. Langelaan, and B. Cheng, "Bio-inspired inverted landing strategy in a small aerial robot using policy gradient," in *IEEE/RSJ International Conference on Intelligent Robots and Systems (IROS)*, 2020, pp. 7772–7777.
- [35] J. A. Andersson, J. Gillis, G. Horn, J. B. Rawlings, and M. Diehl, "CasADi: a software framework for nonlinear optimization and optimal control," *Mathematical Programming Computation*, vol. 11, no. 1, pp. 1–36, 2019.
- [36] K. P. Valavanis and G. J. Vachtsevanos, *Handbook of unmanned aerial vehicles*. Springer, 2015, vol. 1.